Scientia Iranica, Vol. 12, No. 1, pp 75–82

SCIENTIA
IRANICA

Research Note

Optimization of Higher Order Pulse Shapers Used for Reduction of Noise in Amplifier Circuits

M. Tabandeh[1]

Active components in amplifiers generate noise. Thus, amplifiers too, produce noise at their output and, therefore, increase the input signal to noise ratio. This is an undesirable feature, more particularly when one is dealing with weak input signals already combined with noise. Thus, reducing amplifiers' noise becomes a necessity for some applications. To overcome this problem, one approach consists of improving electronic device technology. Another approach is the use of advanced techniques in designing low noise amplifiers by taking advantage of pulse shapers. Pulse shapers generally consist of calculated filters made of integrator(s) and differentiator(s) that limit properly the amplifier bandwidth and, thereby, limit noise through the amplifier. In this study, the effect of variations of parameters of a single differentiator dual integrator pulse shaper on the reduction of noise in an amplifier circuit is investigated and their corresponding values are found for an optimal design.

INTRODUCTION

Active components of a (pre)amplifier produce noise in their output and, therefore, increase the signal to noise ratio existing in their input. The noise sources commonly encountered in electronics are thermal, shot and flicker (also known as $1/f$) noise. More details about noise in semiconductors and the derivation of relevant equations in active elements can be found in [1,2]. As the result of these noises, preamplifiers processing extremely weak signals, such as those coming from sensitive sensors or signal detectors receiving weak signals, have to be designed in such a manner as to have minimum contributions to the original noise in their input signal. Much attention has been given to technology improvement in order to reduce noise in active components [1,3–8].

In this research, the concentration is on pulse shaper parameter optimization to reduce amplifier noise maximally, while giving minimal distortion to the input signal. A pulse shaper usually consists of a filter used in conjunction with the amplifier to limit its bandwidth and, thereby, reduce noise at its output. Figure 1 displays, symbolically, an amplifier with its pulse shaper and the equivalent of voltage and current noise sources referred to its input. For the same reason, they also have an impact on the amplifier output pulse shape. Pulse shapers play a rather important role in reducing noise in amplifiers. Their parameters must, therefore, be calculated in such a way to minimize input signal deformation while reducing maximally the amplifier noise. A well calculated and optimized pulse shaper will thus be of considerable use in decreasing noise.

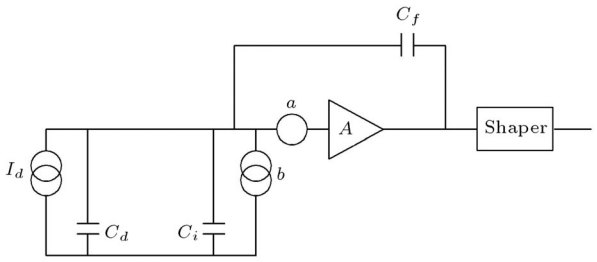

Figure 1. An amplifier circuit with noise sources brought to input.

Evaluation of noise performance of an amplifier circuit has been undertaken by many authors [4,6,9–11]. In these evaluations, the pulse shaper generally consisted of a filter circuit comprising one differentiator and one integrator, both having the same characteristic time constants. However, to the author's knowledge, there has not been a thorough investigation regarding

1. *Department of Electrical Engineering, Sharif University of Technology, Tehran, I.R. Iran.*

the amount of noise reduction when these time constants vary and what their optimal value would be.

In [12], parameters of a pulse shaper for a charge sensitive preamplifier were investigated and it was observed that given the noise parameters of the preamplifier and the detector whose output signal was to be amplified, the total noise at the output of an amplifier depended on the parameters of its pulse shaper (time constants τ_1 and τ_2 of the differentiator and the integrator circuits, respectively). It was also noted that the shape of the corresponding power spectral density curve of the total amplifier noise in the vicinities of its minimum was very flat i.e., changing the time constant of the integrator from about one third to three times that of its optimal value would increase the total equivalent noise charge ($ENC_{\rm tot}$) by about one percent.

In this study, a similar charge sensitive preamplifier circuit is considered consisting of a GaAs MESFET preamplifier with its pulse shaper consisting of one differentiator and two integrators. Pulse shapers with more than one differentiator have been shown to be of little interest [9]. A signal detector is also considered whose output signal is to be amplified. Then, the effect of shaper parameters is investigated on the noise produced at the output of the preamplifier as the result of series and parallel equivalent input noise sources [1].

A charge sensitive preamplifier is a low noise amplifier designed for amplification of signals consisting of charges oncoming generally from a detector and resulting in a voltage swing at the output that starts from zero, passes by a maximum ($V_{\rm out\,max}$) and, then, reclines back to zero. Let us now consider the general form of a charge sensitive amplifier and its pulse shaper circuit as shown in Figure 1. The detectors are generally circuit wise equivalent to their output capacitance and, as one will see, contribute to the amplifier noise. Also, whenever they detect a signal at their input, they deliver a proportional charge to their output (the amplifier input). In the circuit of Figure 1, the amplifier of gain A is assumed noiseless. Noise sources a and b are the equivalent series (voltage) and parallel (current) of the amplifier noise referred to its input [1]. Also, $a(\omega)$ and $b(\omega)$ are their respective spectral power densities. $I_d(\omega)$ represents the parallel noise associated with the detector and its bias circuitry.

The above mentioned noise factors are functions of the types of transistor used in implementation of preamplifiers, as well as their parameters and technology [2,3,13]. Explanation of noises in transistors and derivation of relevant formulas can be found in [1,3,9,14,15]. In this research, since the fast GaAs MESFETs are being used as the preamplifier components, thermal and $1/f$ noise will be dealt with and not the shot noise, since MESFETs do not have junctions[16–19].

In the circuit Figure 1, capacitors C_d, C_i and C_f are the detector, preamplifier input transistor and feedback capacitors, respectively.

If one assumes that the shaper consists of one differentiator and two integrators, then, the open loop transfer function of the preamplifier and the shaper will be:

$$T(s) = \frac{uvAs\tau_1}{(1+\tau_1 s)(1+\tau_2 s)(1+\tau_3 s)}, \tag{1}$$

where τ_1, τ_2 and τ_3 are the time constants associated with the differentiator and two integrators, respectively. A is the preamplifier voltage gain and u and v are voltage gains associated with two integrators. If one sets:

$$\tau_1 = \tau, \quad \tau_2 = \eta_1.\tau, \quad \tau_3 = \eta_2.\tau,$$

then, Equation 1 becomes:

$$T(s) = \frac{uvAs\tau_1}{(1+s.\tau)(1+s\eta_1.\tau)(1+s\eta_2.\tau)}. \tag{2}$$

Now, if instantly or in a very short time, one inserts a charge equivalent of one electron to the input of the circuit, the resulting voltage produced at the output of pulse shaper will be:

$$V_{\rm out} = \frac{uvq}{C_f + \frac{(C_d+C_i)}{A}} L^{-1}[T(s)/s], \tag{3}$$

where q is the electron charge ($1.61 \times 10^{-19} c.$) and C_f, C_d and C_i are capacitors, as described above and $L^{-1}[T(s)/s]$ is the inverse Laplace transform of $T(s)$. One, therefore, obtains:

$$V_{\rm out} = \alpha \left\{ \frac{\eta_1 e^{-t/\eta_1.\tau}}{(\eta_1-\eta_2)(1-\eta_1)} + \frac{e^{-t/\tau}}{(1-\eta_1)(1-\eta_2)} + \frac{\eta_2 e^{-t/\eta_2.\tau}}{(\eta_2-\eta_1)(1-\eta_2)} \right\}, \tag{4}$$

where:

$$\alpha = \frac{uvq}{C_f + \frac{(C_d+C_i)}{A}}.$$

Note that $V_{\rm out}(t)$ starts from a zero value, increases, passes by a maximum and, then, decreases exponentially to zero. The amplitude of $V_{\rm out}(t)$ is then defined as the maximum value of $V_{\rm out}(t)(V_{\rm out\,max})$ reached at a certain time t_m.

In the following section, analytical relations giving the expressions of integrated noise for each type of noise source will be used, namely, thermal and $1/f$ noise. Thermal noise referred to input of the amplifier would be equivalent to voltage (series) and current (parallel) noise sources, as shown in Figure 1. Note that $1/f$ noise has a different spectral power density and has to be treated separately.

NOISE CALCULATIONS

As stated earlier, MESFETs do not have junctions and, consequently, do not generate shot noise. Therefore, in this case, the main sources contributing to amplifier noise are thermal and $1/f$ noise. The effect of thermal noise at the output of amplifiers is modeled and found to be equivalent to voltage and current noise sources placed at the input of them [1]. Therefore, calculations will have to be undertaken for three types of noise source at the input of the amplifier. Details of noise calculation can be found in [1,9]. Only the results of calculations for each type of noise are written here.

a) The a noise:
Consider again the preamplifier circuit of Figure 1. The expression for the total output noise, due to series input voltage noise, is given as:

$$\overline{V}^2_{Na}=\beta\int_0^\infty \frac{\omega^2\tau^2}{(1+\tau^2\omega^2)(1+\eta_1^2\tau^2\omega^2)(1+\eta_2^2\tau^2\omega^2)}df, \tag{5}$$

where $\beta=\alpha.a$ in which a is the voltage of Thevenin equivalent of noise source referred to the input of the amplifier (Figure 1). The value of $\overline{V}^2_{Na}$ is found to be:

$$\overline{V}^2_{Na}=\frac{\beta}{4(1+\eta_1)(1+\eta_2)(\eta_1+\eta_2)\tau}=\theta(\eta_1,\eta_2)/\tau. \tag{6}$$

b) The b noise:
For the preamplifier circuit of Figure 1, the output noise, as the result of the Norton equivalent of noise source with an effective value b at its input, is expressed as;

$$\overline{V}^2_{Nb}=\gamma\int_0^\infty \frac{\tau^2}{(1+\tau^2\omega^2)(1+\eta_1^2\tau^2\omega^2)(1+\eta_2^2\tau^2\omega^2)}df, \tag{7}$$

where $\gamma=\alpha.b$. Evaluating the above expression, one obtains:

$$\overline{V}^2_{Nb}=\frac{\gamma(\eta_1+\eta_2+\eta_1.\eta_2)\tau}{4(1+\eta_1)(1+\eta_2)(\eta_1+\eta_2)}=\nu(\eta_1,\eta_2).\tau. \tag{8}$$

c) The A_f/f noise:
At lower frequencies, this noise is the dominant factor in semiconductor circuits. The output noise produced as the result of this component is expressed as:

$$\overline{V}^2_{Nf}=\delta\int_0^\infty \frac{\tau^2\omega}{(1+\tau^2\omega^2)(1+\eta_1^2\tau^2\omega^2)(1+\eta_2^2\tau^2\omega^2)}df, \tag{9}$$

where $\delta=\alpha.A_f$.

The expression obtained for this noise after carrying the calculations is;

$$\overline{V}^2_{Nf}=\frac{(\eta_1^2-1)\eta_2^2\ln(\eta_2)-(\eta_2^2-1)\eta_1^2\ln(\eta_1)}{(\eta_1^2-1)(\eta_2^2-1)(\eta_2^2-\eta_1^2)}=\xi. \tag{10}$$

ENC COMPUTATION

The noise performances of a preamplifier circuit of the type shown in Figure 1 are generally determined as the amount of Equivalent Noise Charge (ENC) referred to the input of the circuit. This term is defined as the value of an equivalent charge (usually in number of electrons) that, if injected at once to the input of the circuit, would produce a signal amplitude at the output equal to the root mean square of the total output noise of the circuit. Since, as a response to the pulse of a charge insertion, $V_{\rm out}(t)$ would start from zero, pass by a maximum and then fall slowly to zero again, the amplitude of $V_{\rm out}(t)$ will be defined as $V_{\rm out\,max}$ reached at a certain time called t_m.

For more details about ENC definition and calculation, the reader is referred to [9]. Therefore, the total noise at the output of the circuit of Figure 1 is:

$$\overline{V}_{Nrms}=\left[\overline{V}^2_{Na}+\overline{V}^2_{Nb}+\overline{V}^2_{Nf}\right]^{1/2}, \tag{11}$$

and the equivalent noise charge of the circuit, as defined previously, will be:

$$ENC_{\rm tot}=\frac{\overline{V}_{Nrms}}{V_{\rm out\,max}}=\frac{[\theta/\tau+\nu.\tau+\xi]^{1/2}}{V_{\rm out\,max}}, \tag{12}$$

as mentioned earlier, $V_{\rm out\,max}$ is the amplitude (maximum value) of $V_{\rm out}$ that would be produced if a charge of one electron were inserted instantly to the amplifier input. The parameters $\theta(\eta_1,\eta_2),\nu(\eta_1,\eta_2)$ and $\xi(\eta_1,\eta_2)$ have been defined in Equations 6, 8 and 10.

ENC OPTIMIZATION

In Equation 12, $ENC_{\rm tot}$ is noted to be a function of τ,θ,ν and ξ. The latter three being themselves functions of η_1 and η_2 i.e., the ratio of time constants of integrators and the differentiator of the pulse shaper.

Optimization of Equation 12 for the total noise at the output would first require optimization with respect to τ, the time constant of the differentiator, and, then, with respect to η_1 and η_2, simultaneously. The square root term in the numerator of Equation 12 has only two terms that are functions of τ, namely:

$$fl(\tau)=\theta/\tau+\nu.\tau. \tag{13}$$

The particular value τ_o of τ that minimizes fl is the value which would make both terms of Equation 13 equal in value. Thus, one would have:

$$\theta/\tau_o=\nu.\tau_o,$$

therefore:

$$\tau_o=[\theta/\nu]^{12}, \tag{14}$$

and assuming that $\tau = \tau_o$, then one will have:

$$fl(\tau_o) = 2[\theta.\nu]^{1/2}.$$

Therefore, using this value in Equation 12, one obtains:

$$ENC_{\rm tot} = \frac{\{2[\theta.\nu]^{1/2} + \xi\}^{1/2}}{V_{\rm out\,max}}. \tag{15}$$

Now, one has to proceed minimizing this expression, this time with respect to η_1 and η_2. To do this, let one, first, subdivide the expression for the total ENC into two basic noise components, namely, thermal component ($ENC_{\rm th}$) and the contribution of $1/f$ noise (ENC_f). The value of $ENC_{\rm th}$ optimized with respect to τ was found to be:

$$ENC_{\rm th} = \frac{\{2[\theta.\nu]^{1/2}\}^{1/2}}{V_{\rm out\,max}}, \tag{16}$$

and ENC_f term is equal to:

$$ENC_f = \frac{[\xi]^{1/2}}{V_{\rm out\,max}}. \tag{17}$$

An analytical solution for ENC function minimization leading to exact values for η_1 and η_2 is practically impossible, if not extremely tedious and time consuming. Thus, the computer numerical approach for this minimization is used.

A first estimate in analyzing $ENC_{\rm th}, ENC_f$ and $ENC_{\rm tot}$ shows that there is a minimum for $ENC_{\rm th}$ function approximately at:

$$\eta_1 = \eta_2 = 1.$$

Thus, η_1 and η_2 are limited to remain in the neighborhood of 1.

Then, to evaluate the amplitude of $V_{\rm out}(V_{\rm out\,max})$, one has to consider Equation 4, expressing variations of $V_{\rm out}$ with time. This relation is repeated here as the following relation:

$$V_{\rm out} = \alpha\left\{\frac{\eta_1 e^{-t/\eta_1.\tau}}{(\eta_1-\eta_2)(1-\eta_1)} + \frac{e^{-t/\tau}}{(\eta_1-1)(\eta_2-1)} + \frac{\eta_2 e^{-t/\eta_2.\tau}}{(\eta_2-\eta_1)(1-\eta_2)}\right\}. \tag{18}$$

As one can note, $V_{\rm out}$ is a function of t, τ, η_1 and η_2 i.e., for any fixed value of η_1 and $\eta_2, V_{\rm out}$ will only be a function of t/τ. Let one assume that $V_{\rm out}$ takes its maximum value at $t = t_m$. Therefore, t_m/τ will be a function of η_1 and η_2. To find an acceptable approximating equation for it as a function of η_1 and η_2 in the vicinities of 1, the following equation is suggested:

$$t_m/\tau = K_1 + K_2(\eta_1-1) + K_3(\eta_2-1) + K_4(\eta_1-1)^2 + K_5(\eta_2-1)^2 + K_6(\eta_1-1)(\eta_2-1).$$

Expanding the above equation leads to the following form [9]:

$$t_m/\tau = C_1 + C_2(\eta_1+\eta_2) + C_3(\eta_1^2+\eta_2^2) + C_4\eta_1.\eta_2, \tag{19}$$

with the constraint for η_1 and η_2 to remain in the neighborhood of 1. The coefficients C_1, C_2, C_3 and C_4, determined numerically, gave excellent approximations for t_m/τ in the domain of the author's calculations. Numerical values obtained for these coefficients, rounded to four digits, are listed in Table 1.

Figure 2 shows a three-dimensional plot of relative amplitude of $V_{\rm out}(t)$, that is:

$$\text{Amp}(\eta_1, \eta_2) = \frac{V_{\rm out\,max}}{\alpha},$$

for η_1 and η_2 varying from 0.8 to 1.2. Note in this figure that the amplitude function [Amp(η_1, η_2)] is a continuously decreasing function of both η_1 and η_2.

To continue the process, the attention is now focused on two ENCs, namely the thermal term $ENC_{\rm th}$ and the one relevant to flicker ($1/f$) noise, ENC_f:

Table 1. Numerical values obtained for C_1 to C_4.

C_1	0.436
C_2	0.895
C_3	0.224
C_4	0.223

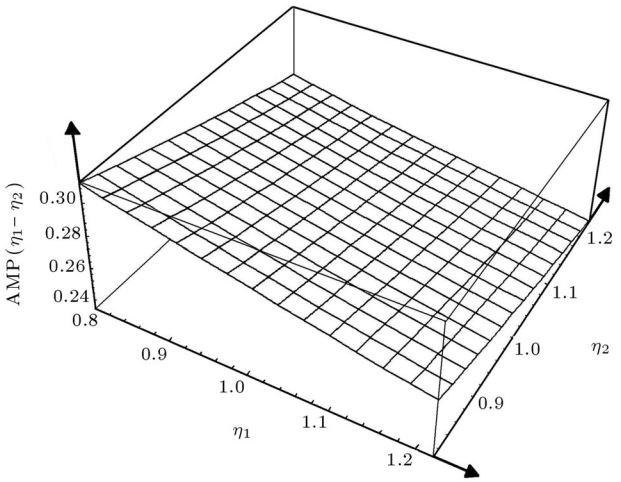

Figure 2. Plot of Amp$(\eta_1, \eta_2) = \frac{V_{\rm out\,max}}{\alpha}$ as a function of η_1 and η_2.

a) The $ENC_{\rm th}$:
Considering Equations 11, 12, 18 and 19 and assuming that τ is chosen to be equal to its optimal value, as given in Equation 14, the expression for $ENC_{\rm th}$ becomes:

$$ENC_{\rm th}(\eta_1,\eta_2) =$$

$$\mathcal{X}\frac{\left[\frac{\eta_1+\eta_2+\eta_1.\eta_2}{(1+\eta_1)^2(1+\eta_2)^2(\eta_1+\eta_2)^2}\right]^{1/2}}{A_1e^{-t_m/\eta_1.\tau}+A_2e^{-t_m/\tau}+A_3e^{-t_m/\eta_2.\tau}}, \quad (20)$$

where:

$$\mathcal{X} = \left[\frac{a.b.C_t^2}{4}\right]^{1/2}/q,$$

$$A_1 = \frac{\eta_1}{(\eta_1-1)(\eta_1-\eta_2)},$$

$$A_2 = \frac{1}{(\eta_1-1)(\eta_2-1)},$$

$$A_3 = \frac{\eta_2}{(\eta_2-1)(\eta_2-\eta_1)},$$

and C_t is the total capacitance seen at the input of preamplifier.

Figure 3 is a three-dimensional plot of $ENC_{\rm th}/\mathcal{X}$. To achieve this calculation, Equation 19 was used for different values of t_m/τ. One can note that the minimum of this function occurs at the vicinities of $\eta_1 = \eta_2 = 1$.

Note that the surface function of Figure 3 becomes very flat in the neighborhood of its minimum. To obtain some idea of its flatness, a plot of the function with contours distant in value, each one by 0.05% of the value of the function and above the minimum, is displayed in Figure 4. As can be seen

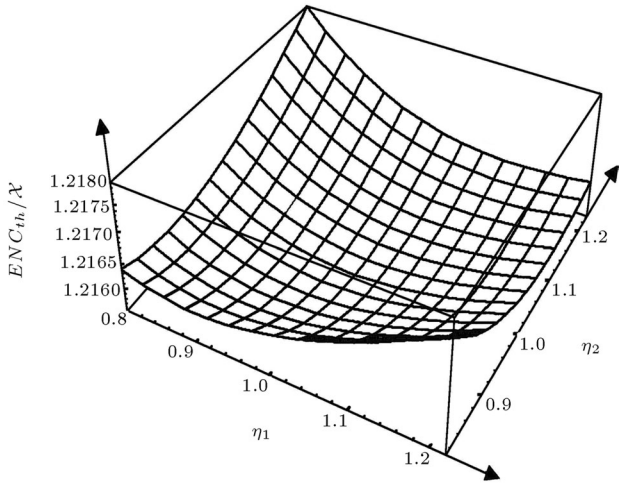

Figure 3. Surface plot of $ENC_{\rm th}/\mathcal{X}$ as a function of η_1 and η_2 approximated in the vicinities of $\eta_1 = \eta_2 = 1$.

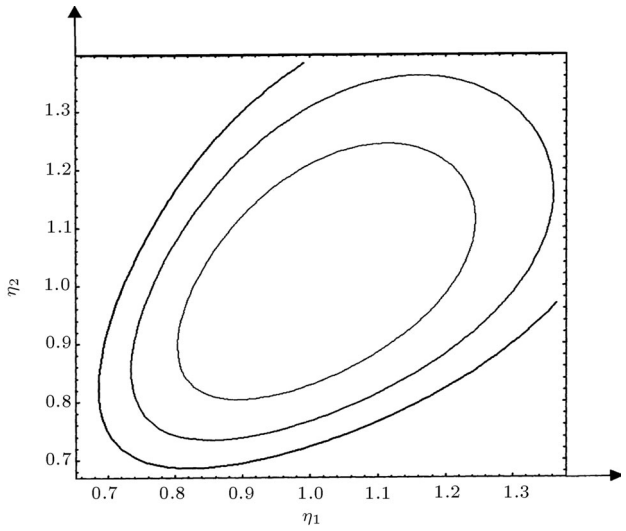

Figure 4. A contour plot of $ENC_{\rm th}$ with contours separated from each other by steps of 0.05% of the value of the function at $\eta_1 = \eta_2 = 1$ and above that value.

in this figure, if one allows the thermal equivalent noise charge ($ENC_{\rm th}$) to take a value less than 0.1% above its minimum and put a constraint on η_1 to remain equal to 1, then, η_2 can vary from 0.76 to 1.3, approximately. Likewise, if one keeps $\eta_2 = 1$, then, η_1 can change within the same limits. If now equality is imposed to two integrator time constants, that is $\eta_1 = \eta_2$, then, the range of their variations will be from 0.78 to about 1.28 for the same tolerance.

b) The ENC_f:
From Equation 10, one can note that the value of $\overline{V}_{Nf}^2$ does not depend on the value of τ. The expression of ENC_f can, then, be written as:

$$ENC_f(\eta_1,\eta_2) = \Delta$$

$$\times\frac{\left[\frac{(\eta_1^2-1)\eta_2^2\ln(\eta_2)-(\eta_2^2-1)\eta_1^2\ln(\eta_1)}{(\eta_1^2-1)(\eta_2^2-1)(\eta_2^2-\eta_1^2)}\right]^{1/2}}{A_1e^{-t_m/\eta_1.\tau}+A_2e^{-t_m/\tau}+A_3e^{-t_m/\eta_2.\tau}}, \quad (21)$$

where $\Delta = A_f.C_t^2/q^2$ (A_f is the $1/f$ noise coefficient of the preamplifier).

The three-dimensional plot of ENC_f/Δ variations versus η_1 and η_2 is given in Figure 5. As can be seen in this figure, the ENC_f/Δ variation surface becomes somehow flat in the vicinities of $\eta_1 = \eta_2 = 1$. It is also evident that this is not a true minimum. The surface seems to slope down toward a lower value in three regions: 1) For $\eta_1 \sim 0.96$ and $\eta_2 > 1.2$; 2) For $\eta_2 \sim 0.96$ and $\eta_1 > 1.2$ (this result was predictable from the first case, since ENC_f/Δ is symmetrical with respect to η_1 and η_2); and 3) In the region where $\eta_1 = \eta_2 < 0.8$. Figure 6 is a level contour plot of ENC_f/Δ around $\eta_1 = \eta_2 = 1$. One of the contours displays the

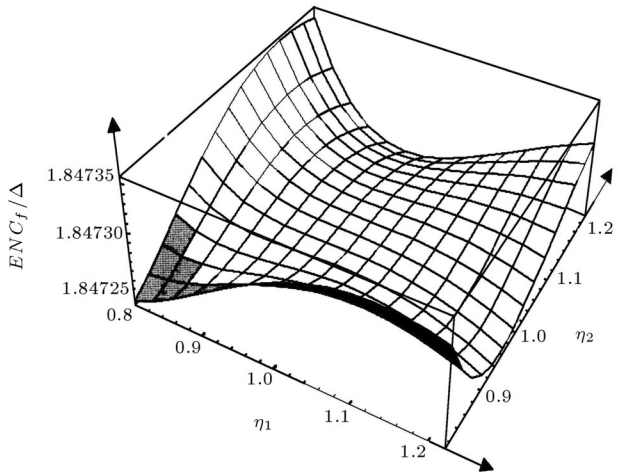

Figure 5. A three-dimensional plot of ENC_f/Δ as a function of η_1 and η_2 around $\eta_1 = \eta_2 = 1$.

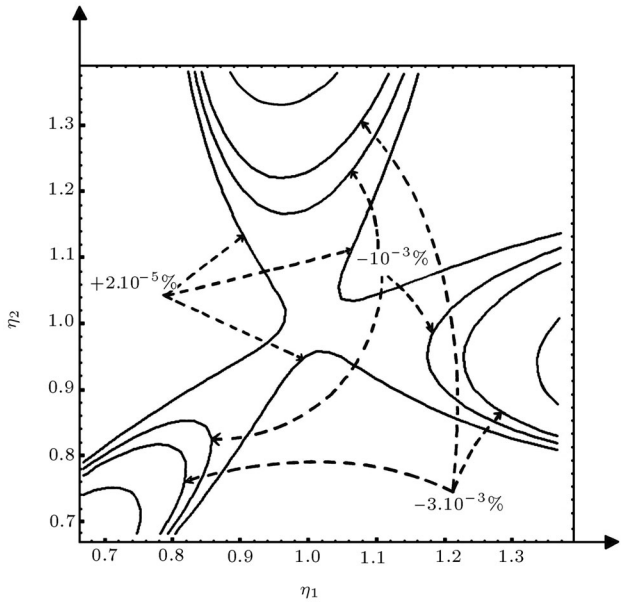

Figure 6. Level contours of ENC_f/Δ for a zone around $\eta_1 = \eta_2 = 1$. The contours have been drawn for values of 0.00002% above the value of the function at $\eta_1 = \eta_2 = 1$ and also for 0.001%, 0.002% and 0.003% below it.

level of 0.00002% above the value of the function at $\eta_1 = \eta_2 = 1, (+2.10^{-5})$, and the other three curves show levels of 0.001% (-10^3), 0.003% and 0.005% below it. These curves also confirm the existence of the three above-mentioned minima for ENC_f/Δ.

Since the function ENC_f/Δ is symmetrical with respect to η_1 and η_2, the behavior of the function was investigated only for η_1 close to 1 and $\eta_2 > 1.2$. The contour plot of Figure 7 displays ENC_f/Δ for values of η_1 in the neighborhood of 1 and $2 < \eta_2 < 3$. This figure shows the existence of a minimum for values of $\eta_1 = 1$ and $\eta_2 \sim 2.5$. Then, η_1 was constrained to remain equal to 1

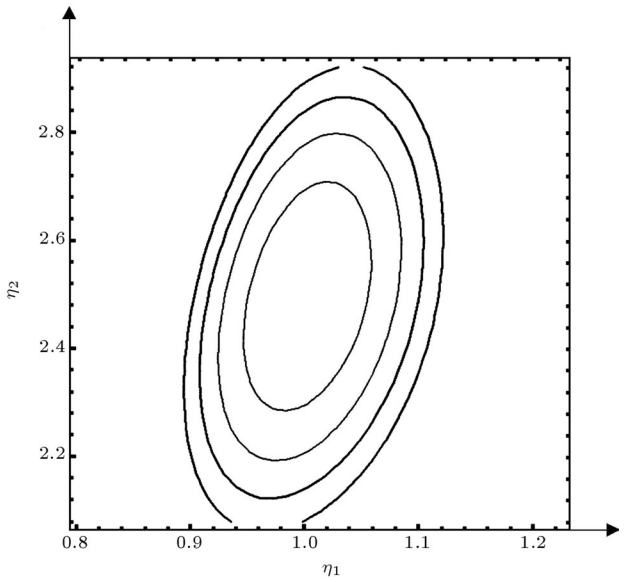

Figure 7. Contour plots of ENC_f/Δ around $\eta_1 = 1$ and $\eta_2 > 2$. Contours are higher by steps of 0.002% of the value of ENC_f/Δ at $\eta_1 = 1$ and $\eta_2 = 2.5$.

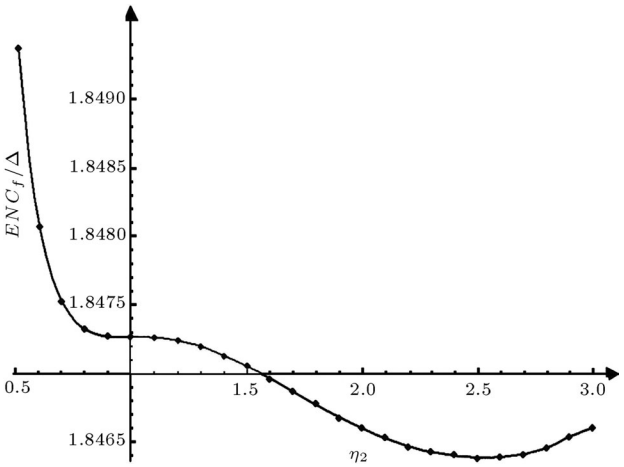

Figure 8. Variations of ENC_f/Δ vs η_2 when $\eta_1 = 1$. Emphasized points are calculated values from analytical form of the function and the curve is a fit to these points.

and variations of ENC_f/Δ were investigated as a function of η_2. Figure 8 displays variations of this function as η_2 goes from 0.5 to 3. On this curve, the emphasized points show the results of direct numerical computations of the analytical form of the function and the curve is a fit obtained to cover these points. Clearly, one can notice the existence of a minimum for $\eta_2 = 2.5$. The numerical value of this minimum of the function is evaluated to be equal to 1.84641. As is also confirmed by this curve, the value of the function is very stable around $\eta_1 = 1$ against variations of η_2 but, of course, it is not a minimum. The second minimum of the function occurs for $\eta_2 = 1$ and $\eta_1 = 2.5$.

For investigating the other minimum in the lower left corner of the contour plot of Figure 6,

$\eta_1 = \eta_2 = \eta$ were made and values of the function were searched for various ηs. Figure 9 shows the variations of ENC_f/Δ for this case. Note again that around $\eta = 1$, the curve becomes flat, but its minimum occurs at $\eta = 0.4$. The numerical value of this minimum of the function is also equal to 1.84641. i.e., practically the same value obtained for the other minimum.

c) The $ENC_{\rm tot}$:
The $ENC_{\rm tot}$ is defined as:

$$ENC_{\rm tot} = [ENC_{\rm th}^2 + ENC_f^2]^{1/2}.$$

The absolute minimum of $ENC_{\rm tot}$, thus, will depend on the coefficients $\mathcal{X}$ and Δ defined previously. If $\mathcal{X} >> \Delta$, then, the most important contribution to $ENC_{\rm tot}$ comes from $ENC_{\rm th}$ and, therefore, its minimum will occur for $\eta_1 = \eta_2 = 1$. If, however, $\mathcal{X} >> \Delta$, then, the main contribution to $ENC_{\rm tot}$ will be due to ENC_f and the absolute minimum will occur for $\eta_1 = 1$ and $\eta_2 = 2.5$ or $\eta_1 = \eta_2 = 0.4$. Generally speaking, if $\Delta = 4.13\mathcal{X}$, then, both minima at $(\eta_1, \eta_2) = (1, 1)$ and $(1, 2.5)$ will have the same value and, if $\Delta > 4.13\mathcal{X}$, then, the absolute minimum of $ENC_{\rm tot}$ will be located only at $\eta_1 = 1, \eta_2 = 2.5$, (the other minimum for $\eta_1 = \eta_2 = 0.4$ will not be acceptable, since $ENC_{\rm th}$ will assume a very high value at this point).

CONCLUSION

In this paper, a pulse shaper (a filter type circuit) used with low noise amplifiers is studied. The parameters of the differentiator, as well as both integrators, have been examined in order to reduce, maximally, the noise power produced by the active elements. At the same time, the narrow bandwidth caused by the pulse shaper should not limit its desired response to input signals from detectors.

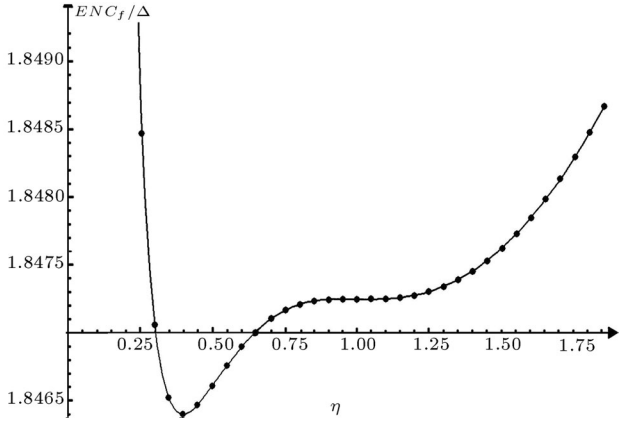

Figure 9. The curve of ENC_f/Δ vs η when $\eta_1 = \eta_2 = \eta$. Emphasized points are calculated values from the analytical form of the function.

In some cases, for an optimum result, the time constants of the integrators, considered variable, were found equal to that of the differentiators. The optimum value of the latter is a function of circuit parameters. For some cases, however, where the output noise is mainly resulted from the input $(1/f)$ noise, two other values were found for the time constants of the pulse shaper integrators, resulting in a minimum noise at the output. The two minima of the output equivalent noise charge (ENC) happened to yield the same value for the function; one was for $\eta_1 = 1$ and $\eta_2 = 2.5$ (or vice versa) and the other for $\eta_1 = \eta_2 = 0.4$.

REFERENCES

1. Howard, R.M., *Principles of Random Signal Analysis and Low Noise Design*, John Wiley & Sons Inc. (2002).
2. Sze, S.M., Ed., *Modern Semiconductor Device Physics*, John Wiley & Sons (1998).
3. Korvink, J.G. and Greiner, A., *Semiconductors for Micro and Nanotechnology- An Introduction for Engineers*, John Wiley & Sons (2002).
4. Abidi, A.A. "On the noise optimum of gigahertz FET transimpedance amplifiers", *IEEE Journal of Solid-State Circuits*, **SC-22**(6), pp 1207-1209 (Dec. 1987).
5. Sansen, W.M.C. and Chang, Z.Y. "Limits of low noise performance of detector readout ront ends in CMOS technology", *IEEE Transaction on Circuits and Systems*, **37**(11) (Nov. 1990).
6. Camin, D.V. et al. "Front end in GaAs", *Nuclear Instruments and Methods in Physics Research A314*, pp 385-392 (1992).
7. Van Der Ziel, A. "$1/f$ noise in HEMT type GaAs FETs at low drain bias", *Solid State Electronics*, **27**(5), pp 375-386 (1983).
8. Duh, K.H. and Van Der Ziel, A. "Hooge parameters for various FET structures", *IEEE Transaction on Electron Devices*, **ED-32**(3), pp 662-666 (March 1985).
9. Gatti, E. and Manfredi, P.F. "Processing the signals from solid state detectors in elementary particle physics", *Editrice Compositori*, Bologna, Italy (1986).
10. Alessandro, A. et al. "Low noise gallium-arsenide charge sensitive preamplifiers for low temperature particle detectors", *IEEE Transaction on Nuclear Science*, **37**(3) (June 1990).
11. Camin, D.V. et al. "Cryogenic charge sensitive preamplifiers for high dynamic range and fast speed Of response using GaAs technology", *IEEE Transactions on Nuclear Science*, **38**(2), pp 53-57 (Apr. 1991).
12. Tabandeh, M. and Venkataraman, S. "Shaper and parameter optimization for low noise amplifiers", I.C.T.P. (Trieste, Italy) Internal Report (Jan. 1994).
13. Streit, D.C. (Chair/Editor) "Gigahertz devices and systems", *Proceedings of the International Society for Optical Engineering*, pp 32-77 (Sept. 1999).

14. Seeger, K. "Semiconductor physics, an introduction", *Springer Verlag*, sixth Ed., pp 115-117 (1997).

15. Weiss, L. and Mathis, W. "A unified description of thermal noise and shot noise in nonlinear resistors", *Proceedings of Unsolved Problems of Noise and Fluctuations*, **511**, pp 89-100 (1999).

16. Hooge, F.N. "40 years of $1/f$ noise modelling", *Proceedings of the Fourteenth International Conference on Noise in Physical Systems and 1/f Fluctuations, World Scientific*, pp 3-10 (1997).

17. Stephany, J.F. "A theory of $1/f$ noise", *Journal of Applied Physics*, **83**, pp 3139-3143 (1998).

18. Peransin, J.M. et al. "$1/f$ noise in MODFETs at low drain bias", *IEEE Transaction on Electron Devices*, **37**(10), pp 2250-2253 (Oct. 1990).

19. Amberiadis, K. et al. "G-R noise spectra of semiconductors and insulators with various trap distributions", *Solid State Electronics*, **33**(7), pp 975-977.